EUROPEAN ORGANIZATION FOR NUCLEAR RESEARCH

CERN-EP/81-130
12 October 1981

The 25-70 GeV Tagged Photon Facility at CERN

Daresbury[1] - Glasgow[2] - Lancaster[3] - Manchester[4] - Rutherford[5] - Sheffield[6] Collaboration.

D. Aston[5], M. Atkinson[5], A.H. Ball[4], G.R. Brookes[6], P.J. Bussey[2], B. Cake[1], D. Clarke[5], K. Connell[1], I.P. Duerdoth[4], R.J. Ellison[4], P.J. Flynn[3], W. Galbraith[6], P.G. Hampson[4], M. Ibbotson[4], R.E. Hughes-Jones[4], M.A.R. Kemp[5], G.D. Lafferty[3], J.B. Lane[4], J. Litt[5], D. Mercer[4], D. Newton[3], C. Raine[6], J.H.C. Roberts[4], K.M. Smith[2], K.M. Storr[3], R. Thompson[4], A.P. Waite[4].

Abstract

A facility which tags the arrival and measures the momentum of photons has been constructed, tested and used in photoproduction experiments with the Omega spectrometer at CERN. The photons are produced by electron bremsstrahlung and are tagged by detecting the scattered electrons. By also measuring the parameters of the incident electron the photon's direction and position at the hydrogen target are reconstructed to ± 70 μrad and ± 2 mm, respectively. The accuracy of the photon momentum determination varies from ± 0.25 GeV/c at 25 GeV/c to ± 0.09 GeV/c at 70 GeV/c. Using a beam of $\sim 2 \times 10^7$ electrons per burst, at a momentum of 80 GeV/c, obtained from 4×10^{12} protons at an energy of 240 GeV, the facility tags $\sim 10^6$ photons in the momentum range 25 to 70 GeV/c.

(Submitted to Nuclear Instruments and Methods)

1. Introduction

In many photoproduction experiments, a precise knowledge of the momentum of the incident photon is of considerable importance. Such a photon facility has been in operation at the Omega Spectrometer at CERN since 1976[1]. Typically 10^6 tagged photons in the momentum range 25-70 GeV/c are produced from an electron beam of 2.10^7 electrons per pulse; the electrons are derived from 4×10^{12} protons incident on a primary target at an energy of 240 GeV. Similar systems have operated at lower energies at electron synchrotrons[2]. A tagged photon beam at FNAL[3] provides photons of higher energy, but no other system provides high momentum photons defined to the same precision described here. This particular system was designed to measure the momentum and the direction of the incident photons to sufficient accuracy to enable four-constraint physics to be realised, using the Omega spectrometer at SPS energies. More recently (1979) a silicon crystal has been used as a radiator in the tagging system to provide a beam of photons whose polarisation is determinable[4]. A full account of the polarised beam will be given in a further paper.

The photon beam is produced by bremsstrahlung. The radiated photon and the scattered electron continue to travel essentially along the direction of the incident electron, angles of bremsstrahlung emission being of the order m_e/E_{INC} where m_e is the electron rest energy. Magnetic spectrometers measure the momentum of the incident (P_{INC}) and outgoing (P_{TAG}) electrons, the difference giving the photon momentum

$$P = P_{INC} - P_{TAG}$$

The photons are tagged in the sense that a fast signal indicates the arrival of a photon within the specified momentum range and this can be used in the formation of the event trigger for the physics investigations. In the subsequent off-line analysis the photon momentum is reconstructed to an accuracy matched to the momentum resolution of the Omega spectrometer. The photon position and its direction at the hydrogen target (at a distance of 21 m from the tagging target) are determined to an accuracy of $\sim$ 2 mm and $\sim$ 70 μrad

respectively, both vertically and horizontally.

The general principles of the tagging facility are described in §2, followed in §3 and §4 by detailed accounts of the two spectrometers. A discussion of backgrounds and corrections is given in §5 while the electronic system for the facility is described in §6. Finally, the performance achieved under experimental conditions is presented in §7.

2. Principles of Operation

The tagged photon beam is a tertiary one. The 240 GeV proton beam of the SPS hits a primary target and produces a secondary beam of photons via the decay of π^0 mesons. Charged particles are swept out of this secondary beam and the photons then produce electron positron pairs in a secondary target. A beam transport system (Fig. 1) (see Ref. 5 for details) selects electrons of a given momentum, normally 80 GeV/c, with a momentum bite, adjustable by collimation, up to $\Delta P/P = \pm 2\%$. The direction of each electron is measured by a series of multiwire proportional chambers (MWPC) distributed along the beam line over the region marked A. A dispersive focus exists within region A so that a position measurement provides a rough determination of electron momentum. The beam then passes through the magnet M1 which provides a bend in the horizontal plane of 68 mrad and removes the dispersion in the beam. The direction of each electron is determined by a set of MWPC's in region B. The momentum of the electron is determined from the trajectories measured in regions A and B. The electrons enter a further magnet, M2, which deflects them horizontally by 9.7 mrad, and steers them onto the tagging target. (M2 is needed to prevent any photons radiated in region B, and further upstream, from entering Omega). Some electrons radiate in the tagging target and the photons continue to the liquid hydrogen target in the Omega spectrometer. The electron beam is focussed by the quadrupoles so that the photons are focussed at the hydrogen target.

The tagging spectrometer comprises the arrangement of magnets and detectors downstream of the tagging target in region C (Fig. 1). The scattered electron is deflected horizontally by the magnets M3 and M4, and a series of MWPC's (WC1...4) enables its trajectory to be determined. The momentum of the scattered electron is calculated from a knowledge of this trajectory, the fields of the tagging magnets (M3, M4) and the electron trajectory through region B. Following the last MWPC are two banks of scintillation counters (HC1, HC2) which provide an approximate determination of the energy of the scattered electron and a time reference for the logic and read-out. Finally, the scattered electron enters an array of lead glass blocks, a signal from which provides confirmation of the identity of a scattered electron. The majority of the incident electrons do not interact in the tagging target, and are deflected by the tagging magnets into the beam dump.

The momentum of the charged particle beam can be varied from 5 to 80 GeV/c and, in addition, it can be tuned to transport predominantly e^-, e^+, π^- or π^+. In the electron mode the pion contamination (which is mostly due to K^0 decay near the primary target) is less than 1%.

The flux of tagged photons is limited both by the large number of primary protons required per photon, and by the rate limitations in the beam spectrometer. The electron intensity increases rapidly with increasing primary proton energy and with decreasing electron energy[5]; in practice the running conditions are a compromise between intensity and energy. Since the total hadronic photoproduction cross-section is only 120 μbarn, it is essential to match the tagging facility with a spectrometer of large solid angle such as Omega, and to use as wide a range of the photon spectrum as possible.

The facility is normally operated at $\sim 2 \times 10^7$ electrons in a spill of ~ 1 s with $P_{INC} = 80$ GeV/c and with the tagging spectrometer covering the electron momentum range 55-10 GeV thus tagging photons with P_γ in the range 25 to 70 GeV/c. The spectrometers can also be operated at reduced fields

to cover other energy ranges, provided that the unscattered electron beam is deflected sufficiently to enter the beam dump.

The next two sections describe the spectrometers in more detail.

3. The Beam Spectrometer

The beam spectrometer consists of MWPC's and scintillation hodoscopes in the regions A and B, together with the intervening beam transport magnets. It has the function of determining the parameters of the electron incident on the tagging target: i.e. its momentum, position and direction (p, y, y', z, z'). In each region the MWPC's determine the position and direction of the straight line trajectory and these are linked using the known transfer matrix of M1. This determines the momentum of the electron relative to the central momentum of the beam. The electron position and direction at the tagging target are then obtained by using the known momentum and the transfer matrix for M2.

The high beam rate ($\sim 2 \times 10^7$ s^{-1}) and the small cross sectional area of the beam (25×30 mm^2) in region A create technical difficulties for the MWPC's. The resulting average rate per wire is $\sim 8 \times 10^5$ s^{-1}, and the rate per unit area is $\sim 2.6 \times 10^4$ s^{-1} mm^{-2}. Particular problems which arise at these high rates include:-

(a) Hits lost due to electronic dead time.

(b) Out-of-time tracks recorded within the coincidence resolving time of the chamber.

(c) Temporary and local loss of efficiency following each avalanche due to space charge effects around the wire.

(d) Permanent degradation of MWPC performance (ageing).

In order to overcome these difficulties 16 planes of MWPC (with 1 mm wire spacing) equipped with special electronics (described below) were distributed throughout each region. The physical sequence of MWPC planes within each region is Y, Z, U, V, Y, Z, U ... where Y(Z) denotes a plane which

measures the horizontal (vertical) co-ordinates, i.e. with vertical (horizontal) wires, and U(V) are planes with wires at + 45^{o} (-45^{o}) to the vertical. To aid pattern recognition, the distance along the beam direction between successive planes of a given orientation is equal within each region. The multi-plane redundancy enables a track to be reconstructed even if several planes fail for any of the above reasons, and also solves the ambiguities which would otherwise arise from the presence of a second track or random background hits. Even if the efficiency per plane is only 85%, the probability of recording at least 10 out of 16 hits still exceeds 99%. The large number of hits reduces the measurement errors on the track sufficiently to give a momentum accuracy of $\sim$ 100 MeV/c for the beam spectrometer. While measurement errors could be reduced by having detectors clustered near the ends of each region this would be less satisfactory for resolving ambiguities in pattern recognition. The MWPC's are a conventional CERN design and the main parameters are given in table 1. Each chamber contains two signal planes with wires at right angles. A 40/60 : Ar/CO_2 gas mixture was used initially, but latterly magic gas has been used successfully. The beginning of the HT plateau for the chambers was 4.9 kV for Ar/CO_2 gas and 4.0 kV for magic gas. Ageing of MWPC's caused problems at the early stages of the experiments. The problems arose as a result of depositions on signal wires and depended upon the gas used. The ageing was manifest in a decrease of gas gain, in operational instability of the chambers and by increasing dark currents. Replacement of the signal wire planes was necessary after some 10^{9} electrons mm^{-2} has passed through the chambers.

To optimise the performance of the beam MWPC's at high rate, especially the pulse pair resolution, low-noise, high-gain fast amplifiers were developed[6]. These have a low impedance grounded based input stage followed by a fast current amplifier. This preserves the shape (20-30 ns FWHM) of the pulses from the chamber. The MWPC's signals must be delayed by approximately 0.8 μs before they can be strobed into readout latches by a suitable trigger from the Omega

spectrometer. This long delay is required partly because the chambers are situated ∿ 70 m upstream of the Omega target and partly because of the transit time through the trigger electronics of the Omega spectrometer. A monostable delay system would introduce an unacceptably long dead time per wire and the obvious alternative of cable delays was therefore used. A pole-zero network shapes the back edge of the amplified MWPC pulse to minimise the overshoot. This is followed by a time-over threshold discriminator, a MECL line driver and about 110 m of twisted pair cable corresponding to a delay of 550 ns (see figure 4). The lay of the twisted pairs in the cable (type BICC PPC 5860,see table 1) is specially designed to reduce the dispersion to ± 2.25 ns and preserve the double pulse resolution of 20 ns. The signals are received from the cable by special modules (called rate gates) which regenerate the MECL signals and strobe them with a logic signal from the tagging system. The tagging pulse indicates that the electron has radiated, but not necessarily that the photon has interacted and caused an event trigger. Since the tagging rate is about 12% of the beam rate, the rate per channel is reduced to about 2.5×10^4 s^{-1}. Lower quality cable can be used for the further delay ∿ 200 ns required before the signals are latched into the CERN RMH[7] readout.

The resolving time of the beam spectrometer is determined at the rate gates. The delay curve had a FWHM of 30 ns and a flat top of 5 ns. The deadtime losses corresponded to ∿ 2.5% for a total electron beam rate of 2.10^7 s^{-1}. (It should be remembered that a jitter of roughly 12 ns is inherent in the chamber signals for 1 mm spaced wires and an electron drift velocity of 25 ns/mm). The loss of efficiency with increasing beam flux has been investigated[8] with these chambers and electronics, and found to be ∿ 5% at a beam intensity of 2×10^7 s^{-1}. The 30 ns coincidence resolving time gives a 45% probability of recording more than one track at this beam intensity. Thus, two scintillator hodoscopes with a coincidence resolving time of 4 ns are included in each region to help in the rejection of out-of-time tracks. The slats of these hodoscopes are 3 mm wide and

0.5 m thick. The space between each MWPC or hodoscope is filled with helium, reducing the total amount of material in each region to 0.027 radiation lengths, corresponding to a multiple coulomb scattering angle θ_{rms} = 0.034 mrad.

The pattern recognition software is identical for the two regions and has to reconstruct the three dimensional track from the hits in up to 16 chambers. It has also to allow for missing hits, additional tracks and random background. The algorithm first finds straight lines separately in each of the four projections, y, z, u, v, demanding that three or four planes have hits. Hits contributing to a 'four hit' event are not used in the search for 'three hit' events. This procedure rejects most of the random background at an early stage, but some spurious lines are still generated. If no line, defined by three or four hits, is present, lines defined by only two hits are included. The wires of the chambers are adjusted to be behind each other to an accuracy of one tenth of the wire spacing and, for the given set of hits, the actual area in phase space (y, y') (z, z') which the line could occupy is considered. The centroid of this phase space is taken as the best estimate of y, y' and the area gives a measure of the accuracy of the measurement. This algorithm can lead to a better accuracy than that given by a least squares fit[9].

The lines in the four projections (y, z, u, v) are used in a least squares fit to give a 3-dimensional track (y, y', z, z'). If this fails, a track is constructed using any three of the four projection and the missing projection is scaled for hits on the resonctructed track.

The above procedures enable more than one track to be reconstructed reliably. An important parameter for each track is the number of hits found on it (varying from 8 to 16) because out-of-time tracks are recorded with reduced efficiency.

The tracks in region A are paired with those in region B using the known momentum-dependent transfer matrix for M1: there are three constraints and one unknown, namely the momentum of the track. If this procedure gives more than one track linking A to B, then the required in-time track can be selected using any of the following methods: a) choosing the track with the most hits in the MWPC's, b) using the additional timing information provided by the scintillation hodoscopes, c) using the information on the secondary electron measured by the tagging spectrometer or d) projecting to the vertex in the Omega hydrogen target.

The electron trajectory is finally projected to the tagging target using the determined momentum, position and direction in region B with the known transfer matrix of M2. Of the five parameters determined viz. p, y, y', z and z', the last four are used in analysis of the secondary electron in the tagging spectrometer, and also give the trajectory of the tagged photon through the hydrogen target. This trajectory is determined to a positional accuracy of about ± 2 mm at the hydrogen target. The vertex position of the interaction in the hydrogen target may be used to refine further the directional information. Some additional corrections have to be applied to the above determination of momentum and are discussed below (§5).

The beam spectrometer determines the energy of the electron approaching the tagging target to an accuracy of ± 100 MeV, and determines its position (in y and z) at this target to an accuracy of ± 0.5 mm and its direction (y' and z') to ± 70 μrad.

4. The Tagging System

The tagging system is called region C on figure 1. The tagging target is mounted on a remote-controlled holder which supports several different targets, any one of which can be placed in position on the electron beam axis. There is also an empty target position on the holder. Under normal running conditions a target of thickness 0.076 radiation lengths was used. Tungsten was chosen for the tagging target because there is some evidence that the bremsstrahlung

spectrum is suppressed in the range, $\sim$ 0.1 to $\sim$ 1.0 MeV/c[10] thus reducing background in the Omega detectors.

The variation in the scattered electron rate with the thickness of the tagging target is shown in figure 2. The extrapolation indicates that the contribution from residual radiators corresponds to 0.0075 radiation lengths. This arises from the windows between the two tagging magnets M3 and M4. Photons radiated here do not, however, have the correct direction to enter the Omega hydrogen target. The magnet M2, the tagging target and the first tagging magnet M3 are under vacuum to ensure that no bremsstrahlung, other than that from the target, can occur within $\pm$ 10 mrad of the line joining the centres of the tagging target and the Omega target. This figure amply exceeds the $\pm$ 2 mrad acceptance of the downstream collimators (§ 5).

Electrons which radiate in the tagging target are deflected horizontally by the dipole magnets M3 and M4 (each approximately 4.5 Tm). The second dipole is a "C" magnet to allow the lower momentum electrons to emerge from the side through the fringe field. The horizontal displacement is approximately proportional to P_{TAG}^{-1}; therefore with constant spatial resolution, high momentum photons are measured more accurately than low momentum photons (associated with the scattered electrons of high momentum). The displacement is measured with MWPC's WC1 ... WC4, the region upstream of WC1 and following M3 being filled with helium gas to minimise effects of multiple coulomb scattering. WC1 to WC4 are all of similar design, each chamber having two signal planes, one with vertical wires and one with wires inclined at 30^{o} to the horizontal. The signal wires (gold-plated tungsten of 20 μm diameter) have spacing of 2 mm. The construction of these MWPC's is such that the electron beam passes through the chambers in a region where there are no sensitive wires. The mean rate of electrons through WC1 ... WC4 in region C is typically only 12% of the rate in regions A and B and is also spread over a larger number of wires. Thus standard CERN RMH read-out is used, without the added complication of delay cables. Ageing of these chambers was also

observed, but they were restored (after $\sim 10^{11}$ electrons had traversed them) by brushing the wires with solvent.

Immediately downstream of WC4 are two scintillation counter hodoscopes (HC1 and HC2) comprising plastic scintillator of thickness 6 mm. HC1 consists of 12 individual scintillator slats of different widths chosen so that each spans approximately the same momentum range. They are useful if an estimate of the momentum is required in the fast trigger. HC2 consists of 16 scintillator slats of equal width (80 mm) which cover the lead glass array (LG). These counters are used to define the time origin of the experimental trigger (see §6 below). Their relative delays are matched to better than 0.5 ns.

The array LG has 3 rows each of 16 lead glass blocks. Each block is 80 mm x 80 mm x 400 mm long (i.e. 13.6 radiation lengths) viewed by a photomultiplier (type RCA6342). Only one row of blocks in LG is used in the experimental trigger at a given time. Radiation damage was observed as a darkening of the glass in the beam plane. This radiation damage, because of the shape of the bremsstrahlung spectrum, is most serious in the lead glass block nearest to the unscattered electron beam, both the energy per electron and the number of electrons per second being largest for that block. Over a 40 day period the light output for this block decreased by $\sim$ 45%. This progressive decrease in pulse height did not prevent the use of LG as a means of discriminating between scattered electrons and hadrons. After approximately 40 days use, or of the order 10^{11} scattered electrons into region C, the row of LG in use was changed by altering the height of the whole array. Figure 3 shows a photograph of the radiation damaged blocks. Blackened blocks were restored by irradiating them with U.V. light.

The lateral positions of HC1, HC2 and LG relative to the beam of unscattered electrons can be adjusted, with corresponding changes in the detection range of scattered electron momenta. Under normal conditions the position is set so that, for an electron beam of momentum 80 GeV/c, scattered electrons of 55 GeV/c to 10 GeV/c can be detected corresponding to tagged

photons of energy 25 GeV to 70 GeV.

Electrons in different parts of the range 10-55 GeV/c traverse very different magnetic fields (those in the range 10-30 GeV/c leave the C type magnet M4 through its side). A full numerical integration along each track would be very expensive on computer time so a fast computational procedure is used. Detailed field maps of the tagging magnets M3 and M4 were used to compute many typical trajectories in the range 10 GeV/c to 55 GeV/c, for various positions and directions of electrons leaving the tagging radiator. It was found that the momentum could be expressed as a polynomial function of three parameters:

(i) the horizontal position of the electron trajectory at the tagging target,

(ii) the horizontal direction of the electron trajectory, at the tagging target,

and (iii) the horizontal position of the scattered electron trajectory at a standard reference plane in region C near to WC4.

Such polynomial expressions for the momentum in terms of these three parameters were found to be sufficiently accurate over each of three overlapping momentum bands. The polynomial coefficients for the computed trajectories are then used for real events. Parameters (i) and (ii) are determined from the MWPC's in region B, and parameter (iii) from the MWPC's in region C.

5. Backgrounds and Corrections

We consider first the various sources of background from radiation and the veto counters used to eliminate them (see figure 1).

(i) Electrons which lose energy prior to bend M1 have their momentum determined correctly but hit the tagging target on the wrong trajectory and give photons in a beam halo. This is eliminated by use of active holey veto counters (HOV 1 and HOV 2) made up of lead scintillator sandwiches. HOV 1 has a hole diameter of 42 mm and defines the photon beam. The

clearing magnet (M5), pairs veto (PV), lead collimator and HOV 2 are designed to eliminate secondary halo produced by interactions at the edge of the hole in HOV 1 which did not trigger that counter. Finally any remaining charged particles in the beam are eliminated by the CV counter.

(ii) As discussed earlier the effect of M2 upstream of the tagging target is to deflect electrons through an angle of 9.7 m radian before reaching the tagging target, whilst leaving photons produced by material ($\sim 2.10^{-2}$ rad lengths) earlier in the beam line undeflected. In order to identify events where such radiation has occurred these undeflected photons are detected in "radiation veto" detector (RV) made up of a total of 24 lead scintillator sandwiches with a total thickness of 16 radiation lengths and an area of 120 mm x 120 mm. Those events in which an energy of $\geq$ 3 GeV is deposited in RV are vetoed; this amounts to 9% of the beam intensity. For smaller energy deposition the measured beam momentum may also, in principle, be corrected by the energy recorded in RV, although there is no need to correct for energies below the resolution of the system ($\sim$ 100 MeV). In practice such corrections are difficult to carry out accurately because of the high rate of photons in this counter.

(iii) The finite thickness of the tagging target gives rise to double bremsstrahlung, or equivalently, to a radiative tail to the measured momentum. The target thickness used in practice is a compromise between intensity and double bremsstrahlung. A "beam veto" counter, BV[11] . situated in the beam behind the Omega spectrometer vetoes events in which a second photon is detected with an energy greater than 3 GeV. Again where a lower energy photon is detected the calculated momentum for the photon triggering the Omega event can, in principle, be corrected by the energy deposited in this counter, although in practice high rates again make this difficult.

(iv) Electrons of momentum 80 GeV/c lose 240 ± 47 MeV/c in synchrotron radiation in the beam transport magnets between A and B. The value of 47 MeV/c is

the calculated RMS magnitude of the statistical fluctuations inherent in the synchrotron radiation process. The spectrometer measures, to a good approximation, the average momentum of the electron along its trajectory through the magnets, and thus a systematic correction of 120 MeV/c is applied to the data. The corresponding loss in M2 is only 27 ± 14 MeV/c and is ignored. Clearly the fluctuation in synchrotron radiation limits the momentum resolution of a tagging system even with ideal detectors.

Table 2 shows the effect of the veto counters on the counting rate in the tagging system. The coincidence rate HC1, HC2, LG has the following contributions:- 9.5% from the tagging target, 0.9% from the vacuum windows between M3 and M4, and approximately 2.5% from those electrons which lose $\gtrsim$ 23 GeV/c of momentum by bremsstrahlung in region B and hence do not need to interact in the tagging target in order to be detected by the tagging system.

RV has two effects:(i) rejecting events where the electron radiates $\gtrsim$ 25 GeV in region B but does not radiate significantly in the tagging target (2.75%) and (ii) rejecting events where the electron radiates $\gtrsim$ 3 GeV in region B and also radiates in the tagging target such that its final energy is less than 55 GeV (0.5%).

The holey veto system eliminates halo due to several causes (i) imperfections in beam optics (hard to calculate), (ii) electrons losing appropriate energy in region A (0.25%) and (iii) electrons losing energy by synchrotron radiation in M2 or M3; thin scintillators CV and PV in the beam eliminate e^+ or e^- of various energies produced in windows or other material.

6. Electronic Logic, Readout and On-line Monitoring

Figure 4 shows a simplified diagram of the logic and timing of the pulses with respect to the time at which a photon crosses the centre of the Omega hydrogen target. The aim of the logic is to provide a signal as early in time as possible, indicating that a tagged photon has been produced. Speed is essential to provide a clean strobe in time with the signals from

the trigger MWPC in the Omega detector. This is achieved by providing a quick signal (QT) from the coincidence of HC1 and HC2, followed later by the full tag signal (FT). The delay between the QT and FT is due to the arrangements of the detectors and counting rooms. The QT, suitably delayed, is used to strobe the rate gates in the beam MWPC readout and strobed coincidence units in the beam hodoscope readout, to reduce the rate per element. An intermediate trigger from the Omega electronic logic is used in coincidence with FT to strobe the RMH and CAMAC systems. If no final trigger resulted from the Omega logic, a fast reset signal cleared the readout.

As discussed earlier long cable delays are used between the amplifiers and the readout of the beam chamber in order to bring MWPC pulses from regions A and B into coincidence with those from detectors further downstream. The minimum electrical length imposed by the physical distances between the detectors and the electronics is indicated by the double line in figure 4. As noted earlier, the time of all coincidences is determined by the leading edge of the HC2 pulse. The leading edge of this pulse is then used to define the timing of all coincidences thereafter i.e. QT, FT and all strobe pulses for the MWPC signals.

The data acquisition system used at Omega involved several PDP computers[12]. Several on-line tasks were used to monitor the operation of the tagging system. Wire distributions for the MWPC's and slat distributions for the hodoscopes were available, together with a list of chamber efficiencies; error messages were produced when, for example, a chamber plane or hodoscope had no hits for several consecutive events. Figure 5 shows a display obtained from the beam MWPC's, of the phase space occupied by the electron beam in regions A and B. These, together with an on-line projection of the beam from region B to the Omega target, proved invaluable in adjusting the beam optics.

7. Performance of System: Experimental Results

In assessing the overall performance of the tagging system, we consider the following effects: (a) the 'quality' of the tagged photon, as recorded by the response of the various elements in the system, (b) the reproducibility of the bremsstrahlung spectrum, and (c) the accuracy with which the absolute value of the momentum of the photon is determined and the momentum resolution achieved by the system including Omega.

(a) The quality of tagged photon is categorised by the off-line analysis as defined in Table 3. The purpose of this photon category "flag" is that, for some of the physics analysis of the data, it is important to use only events for which the photon energy and direction are accurately determined. The figures on table 3 are at a beam intensity of 6×10^6 electron per pulse.

(b) As an occasional monitor during the experimental data taking, the bremsstrahlung spectrum was recorded by switching out the trigger from the Omega spectrometer and allowing the experimental trigger for data recording to be the signal for a tagged photon. An example of such a spectrum is shown in figure 6 and is in agreement with a $1/p_\gamma$ shape (shown) and also with the Tsai and Van Whitis formulae [12] for bremsstrahlung from a thick target. The spectrum of figure 6 is derived from measurement of the scattered electrons, and takes no account of any contribution from double bremsstrahlung in the tagging target. The reduction of the photon yield outside the range 25 to 70 GeV/c is due to the acceptance of the region C detectors.

(c) Several methods have been adopted to investigate the accuracy of the tagging system's determination of the photon momentum.

(i) It is possible to find the directional accuracy of measurements in region B, by turning off the tagging magnets and the Omega magnet, removing the tagging target, and allowing a charged pion beam to pass through the system into the drift chambers located downstream

of the Omega magnet (see figure 1). The drift chamber measurements linked with the track position in region B give a precise measurement (± 20 μrad of track direction). The standard deviation of the error on the region B determination of the track direction by this method was found to be 60 μrad. As an alternative approach, the error matrices for the region A and B track parameters have been calculated from the standard deviation of the individual MWPC measurement, which were assumed distributed as a top hat function over one wire spacing. Under normal conditions, the error calculated for the track direction in region B are 50 μrad, in very good agreement with the error determinated by the drift chamber method.

(ii) Information on the accuracy of the whole tagging system has been obtained experimentally by adjusting the beam line and beam spectrometer to transport pions of various momenta between 10 and 55 GeV/c, removing the tagging target and detecting the pions in region C. Pions were used in preference to electrons in order to eliminate radiative corrections. The width of the distributions of the difference between the momenta measured in the beam and tagging spectrometers are plotted in Fig. 7 as solid circles after correcting for the different absolute errors in the beam momentum measurements caused by the different nomimal beam momenta. The dashed line in Fig. 7 corresponds to the error on the photon momentum calculated by propagating the full track error matrices (discussed above) through the standard calculation of the tagged photon momentum. The agreement with the pion data is very good. At low photon momenta, the error is dominated by the tagging spectrometer but with increasing momentum this error falls leaving the beam spectrometer as the dominant error at the highest momenta.

(iii) The momentum of the tagged photon has been compared directly with momentum measurements in the Omega spectrometer. The most favourable reaction is $\gamma p \to \rho^0 p$ with $\rho^0 \to \pi^+\pi^-$ because it is easily identified and because the recoil proton takes little energy. Electron-positron pair production is less favourable because of difficulties in vertex definition resulting in increased errors in the Omega measurements and because of errors due to bremsstrahlung losses by the e^+ or e^- as they traverse the Omega detectors. Hence ρ^0-mesons were reconstructed and the energy difference $\Delta E = p_\gamma - (E_{\pi+} + E_{\pi-})$ computed and plotted as a function of p_γ. The width of the ΔE distribution is the convolution of the contributions for the tagging system resolution and the Omega resolution. The open circles on Fig. 7 show these data. It is not easy to get an accurate absolute value for the Omega error, but the prediction of the variation of the Omega error with momentum is expected to be reliable. Clearly at high p_γ the error is dominantly due to Omega so we show the predicted variation in Omega error normalised to our high energy data, as the dotted line on fig. 7. This normalisation is consistent with absolute estimates of the Omega momentum resolution. Finally we take the predictions of the two errors from the dotted and dashed curves and by adding these in quadrature get the solid line shown in fig. 7. This solid line is to be compared with the open circle data points. Again the agreement is satisfactory.

Thus the tagging system has a momentum resolution varying between ± 0.25 GeV at 25 GeV/c to ± 0.09 GeV at 70 GeV/c. The use of the vertex position in Omega to constrain the fits slightly improves the momentum resolution of the system for low photon momenta.

8. Summary

A tagging system giving a photon momentum resolution of ± 0.25 GeV decreasing to ± 0.09 GeV between its momentum limits of 25 GeV/c and 70 GeV/c has been operational in conjunction with the Omega spectrometer at CERN. The system operates at intensities up to 2×10^7 electrons per pulse and has a high event reconstruction efficiency. A series of experiments have been carried out showing that the whole device is reliable and useful for an important number of investigations into the nature of photon interactions.

ACKNOWLEDGEMENTS

We express thanks to members of the OMEGA group, and of the SPS and DD Divisions at CERN, for their generous help in setting up this facility. In this connection, we are particularly grateful to D. Plane for the detailed design of the electron beam.

The contribution of the technical staff at our home institutions has been invaluable in the construction of hardware, as has been the generous help given to us by other staff at Daresbury Laboratory and Rutherford Laboratory. Our colleagues from the University of Bonn built the beam veto counter and we wish to express our appreciation to them.

We thank the Science and Engineering Research Council for their support.

Finally, we are grateful for the considerable contribution made by our late colleague, J.G. Rutherglen, of the University of Glasgow, to the design and practical realisation of this tagging facility.

REFERENCES

1. D. Aston et al., Nucl. Phys. B166 (1980), 1.
2. G.R. Brookes et al., Nucl. Instr. Meth. 85 (1970), 125.
   G.R. Brookes et al., Nucl. Instr. Meth. 115 (1974), 465.
3. D.O. Caldwell et al., Phys. Rev. Lett. 40 (1978), 1222.
4. P.J. Bussey et al, Proc. Int. Symposium on High Energy Physics with Polarised Beams and Polarised Targets, Lausanne (1980).
5. D.E. Plane, CERN/SPS/76-1 (1976).
6. B. Cake, Daresbury Laboratory, Internal Report, DL/CSE/TMS (June 1977).
7. RMH Type 4236, Prov. Spec. CERN NP Division (1975).
8. I.P. Duerdoth et al, Nucl. Inst. Meth. 129 (1975), 461.
9. V.D. Drijard et al., Nucl. Instr. Meth. 176 (1980), 389.
10. A.A. Varfolomeev et al., JETP, 42 (1976), 218.
11. M. Dorn, University of Bonn Internal Report, BONN-IR-79-39.
12. D. Botterill, Nucl. Instr. Meth. 166 (1979) 541.
13. Y.S. Tsai and V. Whitis, Phys. Rev. 149 (1966), 1248.

TABLE 1

BEAM MWPC

Active area	100 × 100 mm^2
Signal wire spacing	1 mm
Signal wire diameter	10 μm
Spacing between signal and high voltage planes	5 mm
High voltage plane (aluminium) thickness	10 μm

AMPLIFIERS - DISCRIMINATORS

Input impedance	50 Ω
Input threshold adjustable	0.5-10 μA
Bandwidth	100 MHz
Time slew 2 × to 20 × threshold	4 ns
Dead time for 10 × overdrive	≤ 20 ns

BICC PPC 5860 cable (32-way twisted pair)

Propagation velocity	4.95 ns m^{-1}
Rise time 5% to 50% for 100 m	5 ns
Dispersion (peak to peak)	4.5 ns
Cross talk	≥ 30 dB

TABLE 2

Percentage Coincidence Rates per Beam Electron
(for radiator of thickness 0.076 Xo)

Trigger	Rate %
HC1.HC2.LG	12.6
HC1.HC2.LG.$\overline{RV}$	9.3
HC1.HC2.LG.$\overline{RV}$.$\overline{HOVT}$	8.3
HC1.HC2.LG.$\overline{RV}$.$\overline{HOVT}$.$\overline{HOV2}$	7.8
HC1.HC2.LG.$\overline{RV}$.$\overline{HOVT}$.$\overline{HOV2}$.$\overline{CV}$.	7.4
HC1.HC2.LG.$\overline{RV}$.$\overline{HOVT}$.$\overline{HOV2}$.$\overline{CV}$.$\overline{PV}$.	6.9

TABLE 3

Categories of Tagged Photons

	Category	% of events in Cat.
1.	unambiguous results from regions A, B and C.	74
2.	poor match between track found in region B and that found in region C.	4
3.	ambiguous or no result from regions A and B. The central value of 80 GeV is used for the incident electron energy and the direction is assumed to be on the beam axis.	6
4.	ambiguous or no result from region C, rescue using HC1, HC2 and LG.	13
5.	unable to reconstruct the tagged photon energy.	3

FIGURES

1. Schematic arrangement of the tagged photon beam. (Note the horizontal and vertical scales are different on this figure).
2. Scattered electron intensity as a function of the thickness of the tagging target. The point A is the equivalent thickness of radiator with no tagging target. It is 0.75% of a radiation length.
3. Radiation damage in lead glass blocks.
4. Block diagram of electronic logic for the tagging system.
5. On-line phase space plots for the electron beam.
6. Measured bremsstrahlung spectrum from the tagging system.
7. Momentum resolution of the tagging system. Open circles are the convolution of the resolution of the tagging system and Omega for ρ-photoproduction. Solid circles are the resolution of the tagging system derived from prior data. The dashed line is the calculated tagging resolution, the dotted line is a normalised Omega resolution and the solid line is the predicted overall resolution of the combined system.

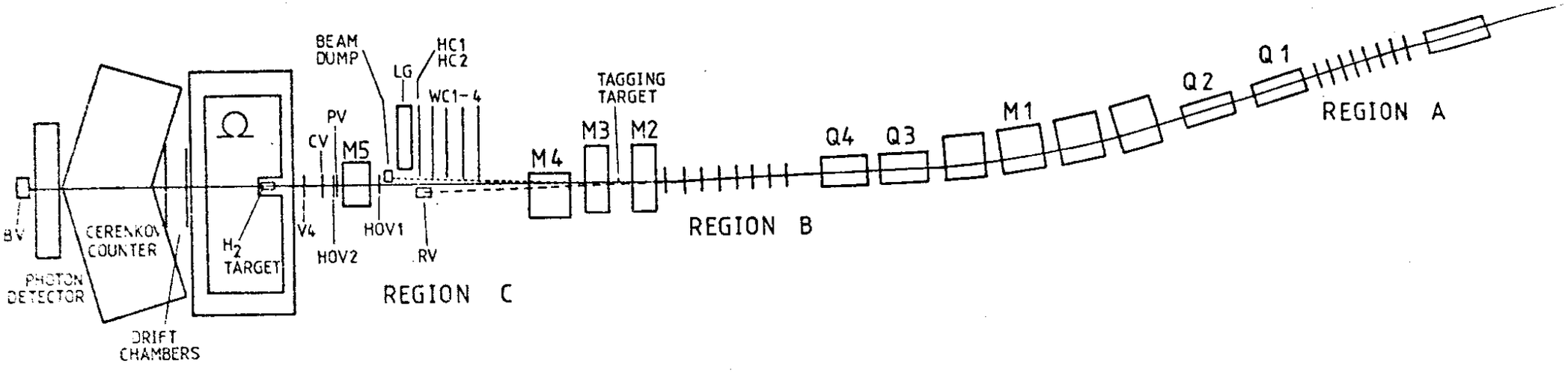
BEAM
DUMP
HC1
HC2
LG
WC1-4
TAGGING
TARGET
PV
CV
M5
M4
M3
M2
Q4
Q3
M1
Q2
Q1
REGION A
BV
CERENKOV
COUNTER
H2
TARGET
V4
HOV1
HOV2
RV
REGION B
PHOTON
DETECTOR
DRIFT
CHAMBERS
REGION C

Fig. 1

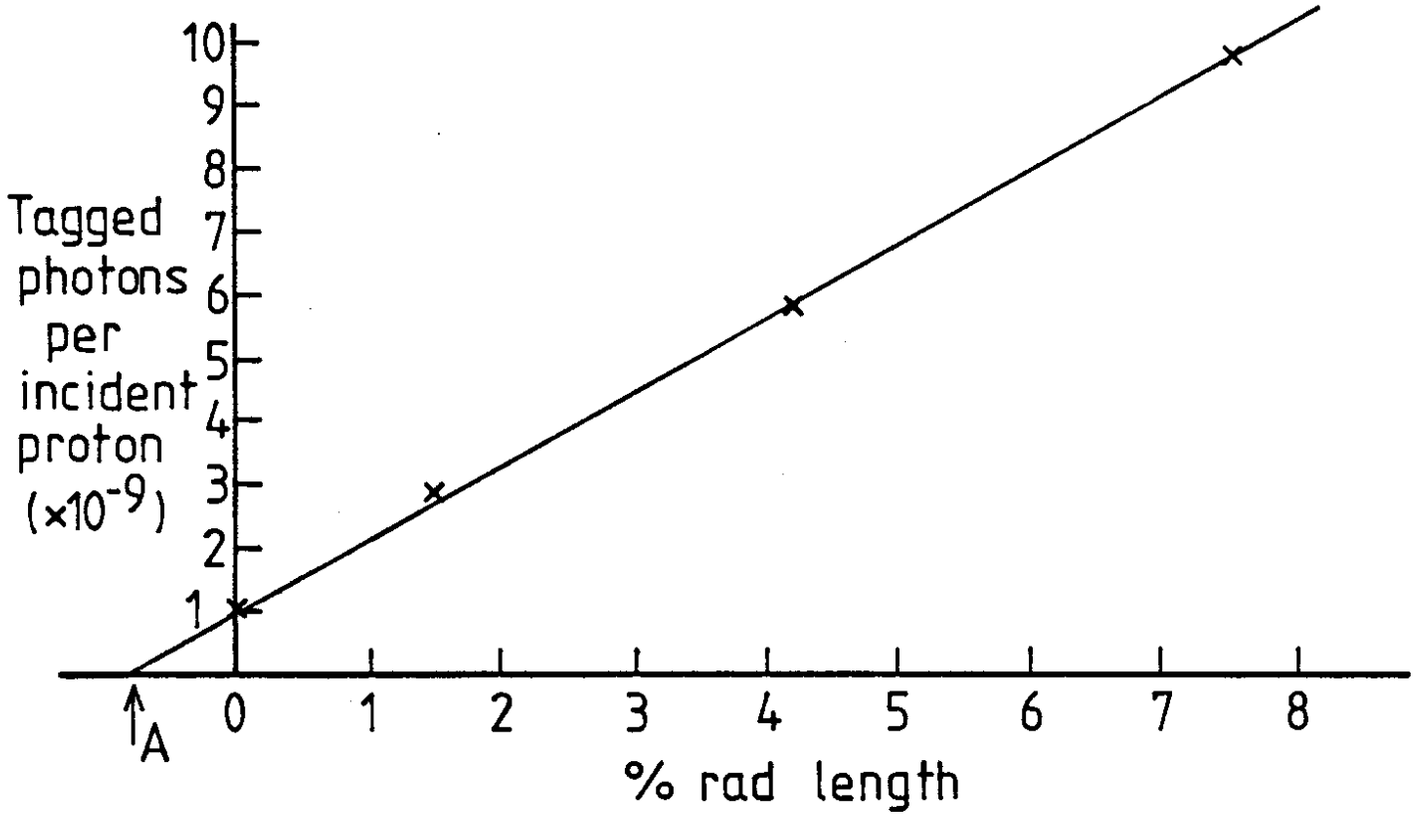
Tagged photons per incident proton (×10⁻⁹)
10
9
8
7
6
5
4
3
2
1
A
0
1
2
3
4
5
6
7
8
% rad length

Fig. 2

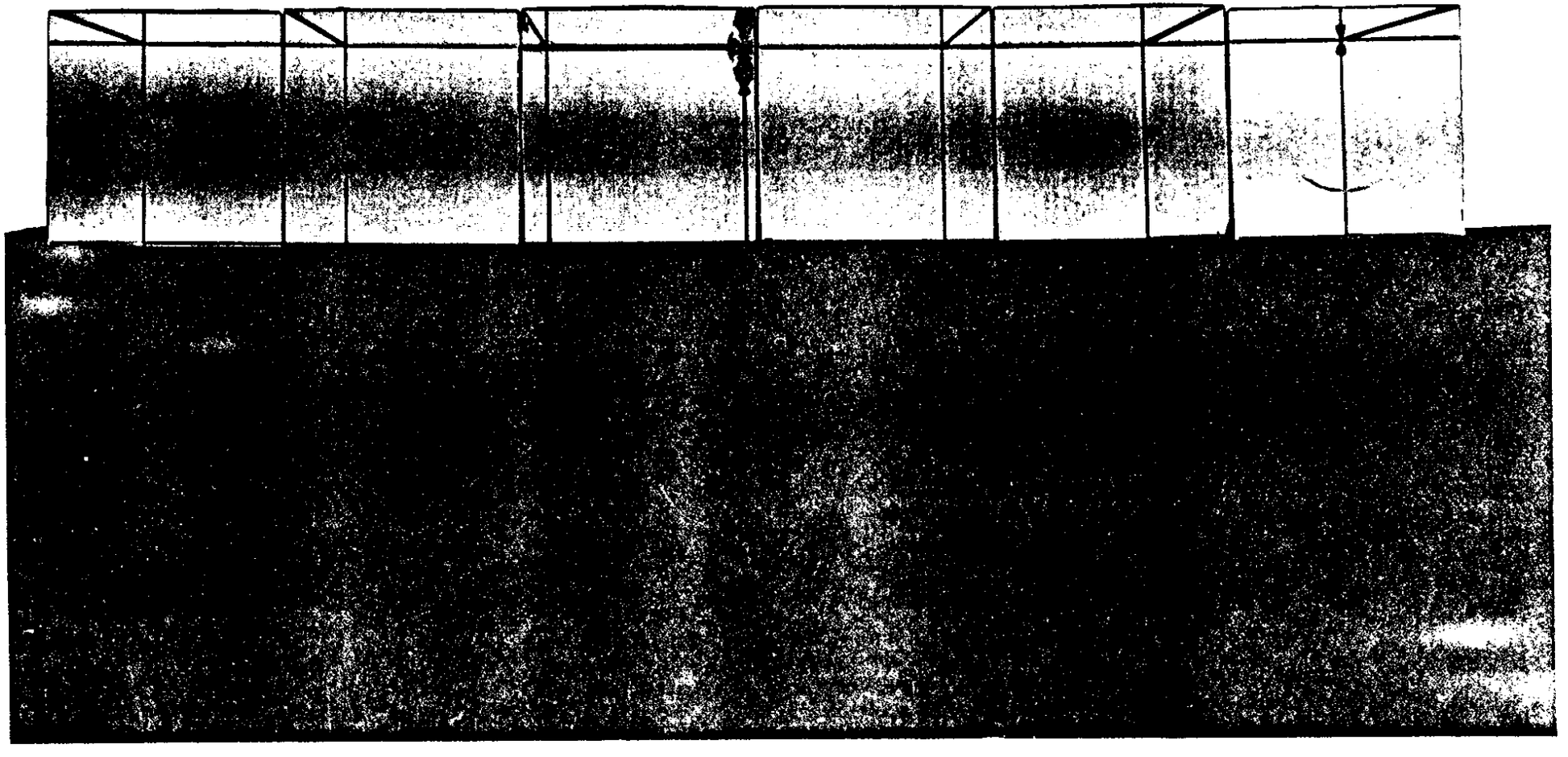

Fig. 3

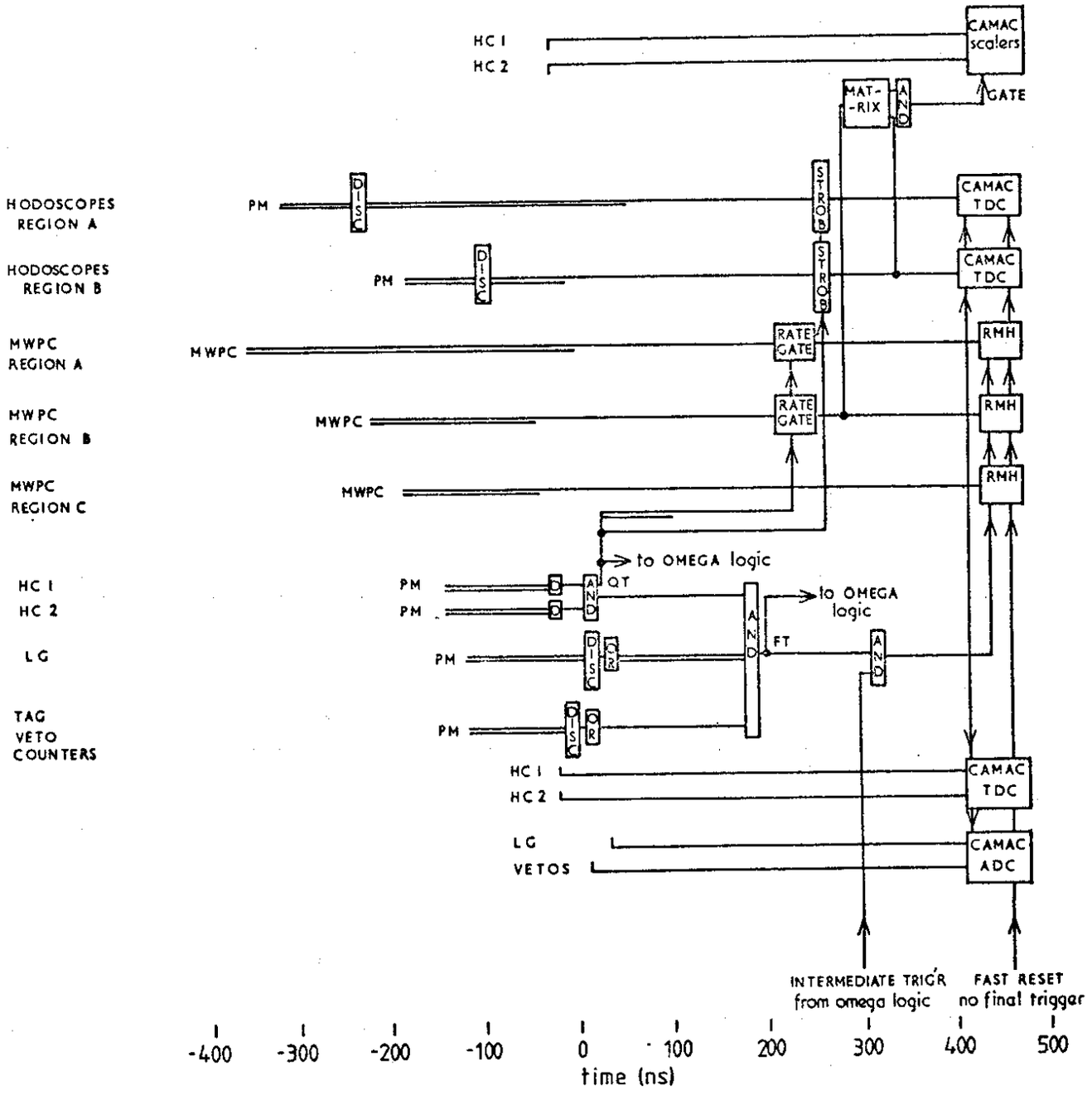
HC 1
HC 2
CAMAC scalers
GATE
MAT-RIX
AND
HODOSCOPES REGION A
PM
DISC
STROB
CAMAC TDC
HODOSCOPES REGION B
PM
DISC
STROB
CAMAC TDC
MWPC REGION A
MWPC
RATE GATE
RMH
MWPC REGION B
MWPC
RATE GATE
RMH
MWPC REGION C
MWPC
RMH
to OMEGA logic
HC 1
HC 2
PM
PM
DISC
AND
QT
AND
to OMEGA logic
LG
PM
DISC
OR
FT
AND
TAG VETO COUNTERS
PM
DISC
OR
HC 1
HC 2
CAMAC TDC
LG
VETOS
CAMAC ADC
INTERMEDIATE TRIG'R from omega logic
FAST RESET no final trigger
-400
-300
-200
-100
0
100
200
300
400
500
time (ns)

Fig. 4

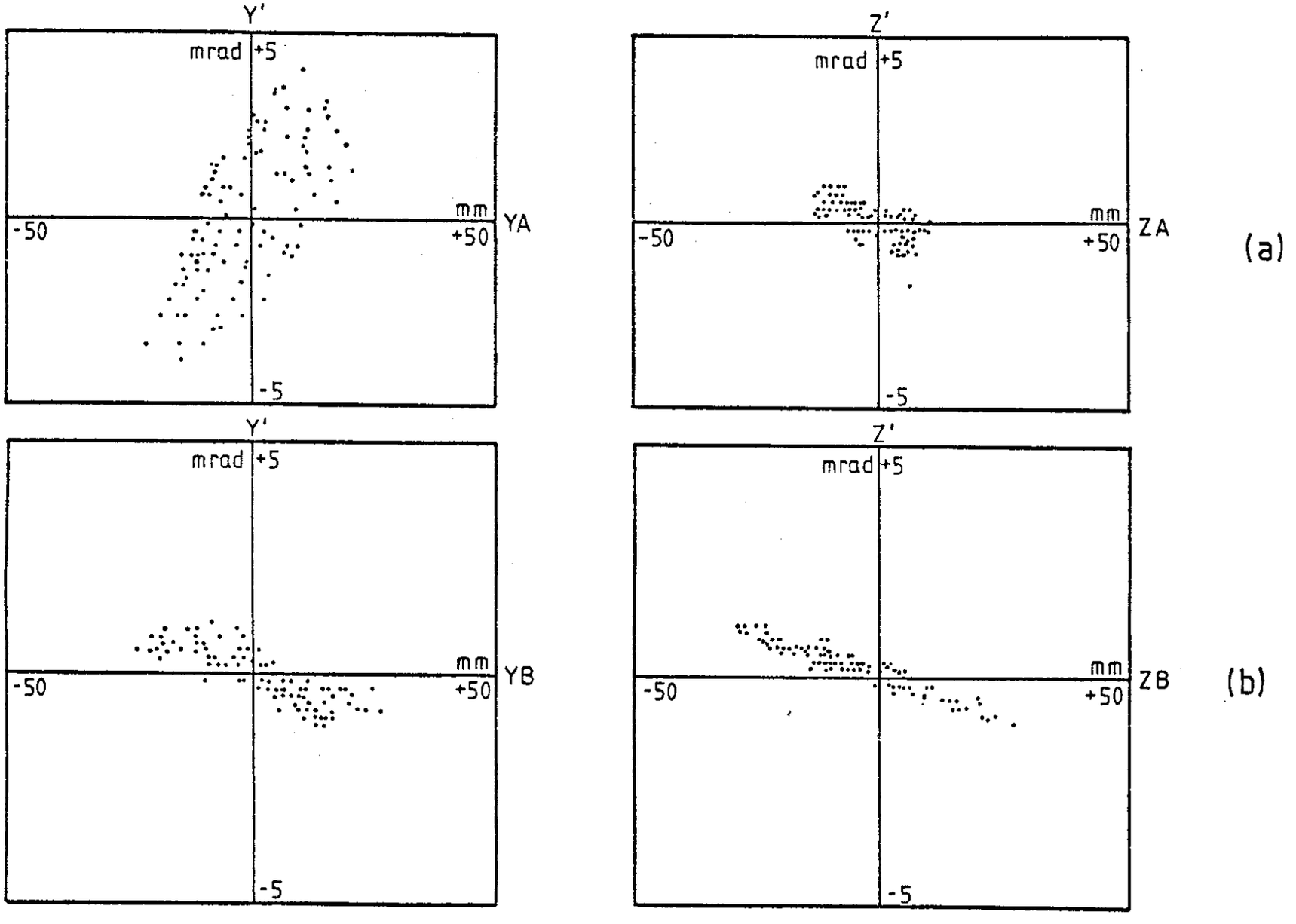
Y'
mrad +5
mm
-50
+50
YA
-5
Z'
mrad +5
mm
-50
+50
ZA
-5
(a)
Y'
mrad +5
mm
-50
+50
YB
-5
Z'
mrad +5
mm
-50
+50
ZB
-5
(b)

Fig. 5

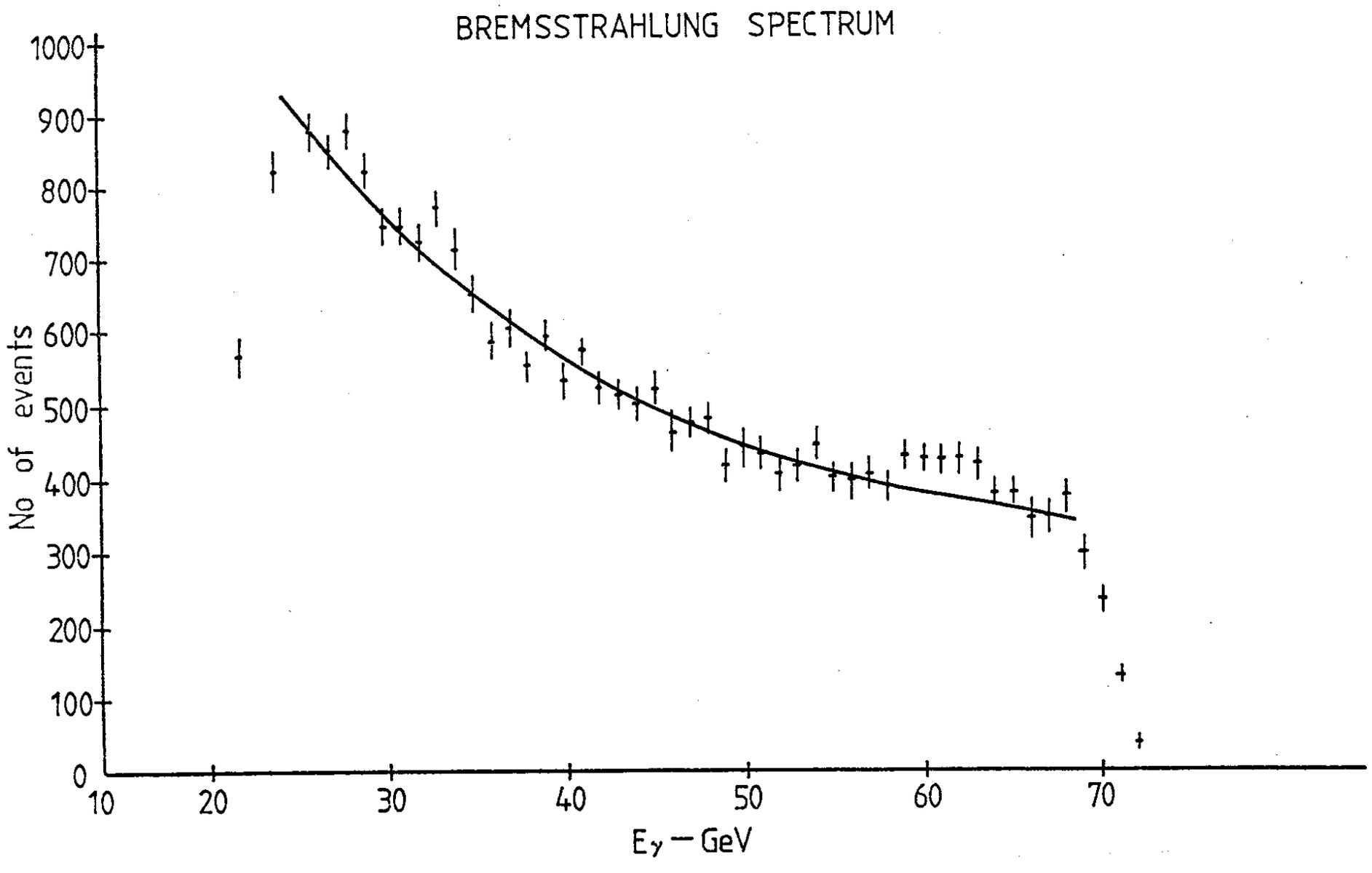
BREMSSTRAHLUNG SPECTRUM
No of events
1000
900
800
700
600
500
400
300
200
100
0
10
20
30
40
50
60
70
Eγ — GeV

Fig. 6

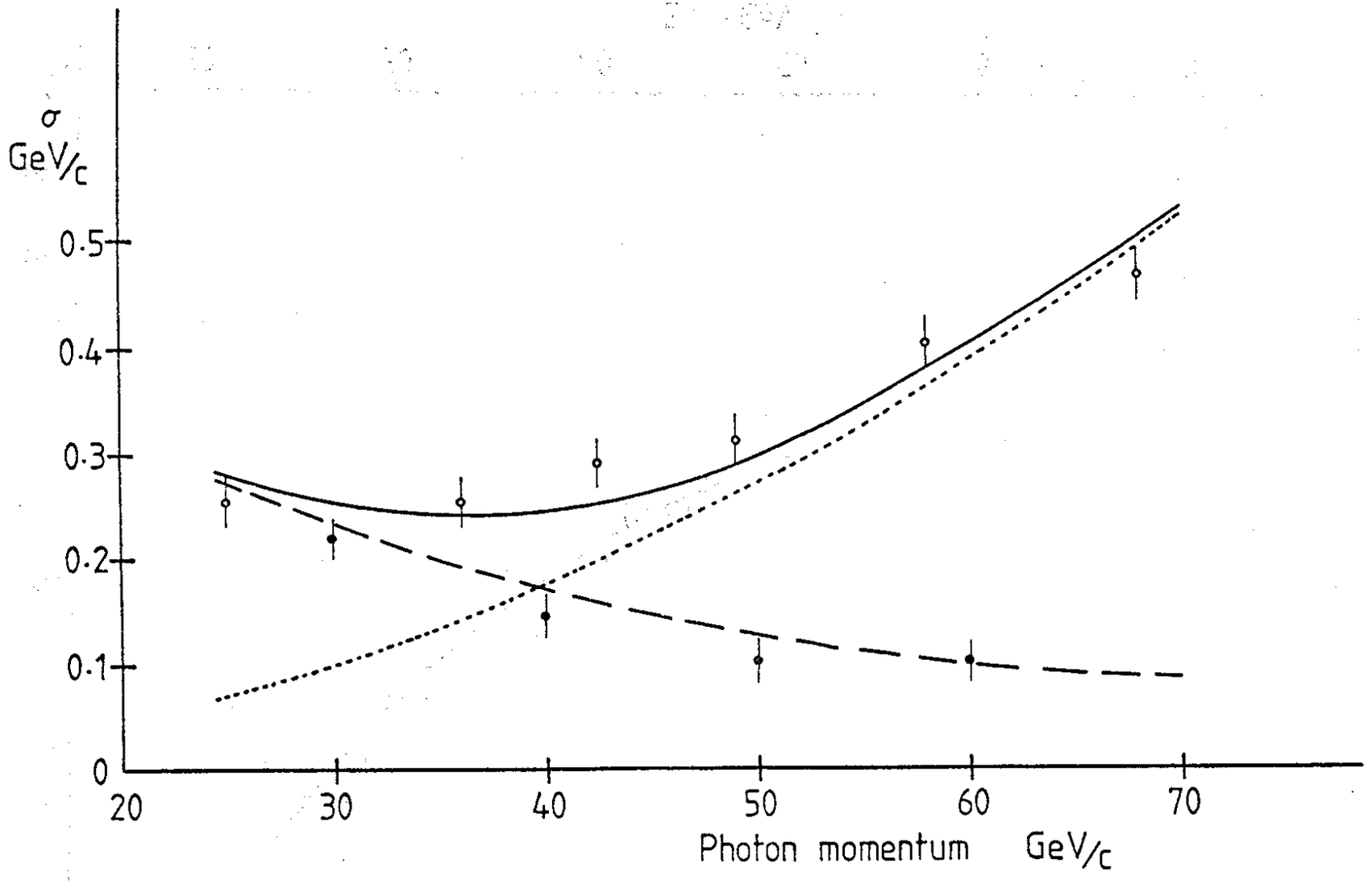

Fig. 7